ISSN 2522-9400 **European Modern Studies Journal** *Vol 7 No 6*
available at www.journal-ems.com
DOI: 10.59573/emsj.7(6).2023.10

Optimum Biodiesel Production from African Oil Bean Seed Oil Using Antelope Bones and Africa Oil Bean Seed Pod as Catalyst: RSM and ANN as Optimization Tools

Kessington Obahiagbon[1], David Ohimai Ahonkhai[1]*, Richard Omoregie[1], Paul Eloke[2]
[1]Department of Chemical Engineering, University of Benin, Benin, Nigeria
[2]Department of Civil and Structural Engineering, Teesside University, Middlesbrough, United Kingdom

Abstract. Heterogeneous catalyst developed from antelope bones and African oil bean seed pod was used for the production of biodiesel from African oil bean seed oil (AOBSO) characterized by 2.22% free fatty acid (FFA) via transesterification reaction. Characterization showed that the catalyst had high surface area (40.65m^2 /g) and large pore diameter (50.85 Å) with CaO being its main constituent. Four independent process variables were optimized using response surface methodology (RSM) and Artificial Neural Network (ANN). The optimization result revealed that a maximum biodiesel yield of 93.25% was achieved using RSM at an optimum condition of temperature (60^{o}C), time (86 minutes), methanol:oil ratio (12:1) and catalyst loading (2 wt.%). Also, using ANN modelling, an optimum yield of 95% was obtained at a temperature, time, methanol:oil ratio and catalyst loading of 57^{o}C, 57 minutes, 7.5:1 and 1 wt.% respectively. The result shows that ANN was better tool at modelling the process because of its higher R^2 value and lower RMSE value. Also, the high yield of biodiesel obtained showed that African oil bean seed oil (AOBSO) which is a low-cost feedstock have the potential to be used for biodiesel production.

Keywords: African oil bean seed, Bone, Optimization, Biodiesel, Renewable energy

Introduction

Energy today occupies a prominent place in the daily lives of humans universally. This has motivated the search for environmentally friendly and sustainable alternatives. Biofuels have been identified as one of such alternatives that can help meet global energy demand without the negative consequences associated with the use of fossil-based fuels (Adekunle et al., 2020; Odetoye & Amusan, 2019).

The depletion of the world's petroleum reserves, global warming and environmental degradation caused by exploration of oil and flaring during production of petroleum products calls for alternative energy sources to petroleum based fuels and the possible alternative to fossil fuels are biofuels which are renewable, non-toxic, safer to handle, biodegradable, requires no engine modifications and reduces dependency on fossil fuels (Ogunsola et al., 2022; Okonkwo et al., 2023).

Biodiesel is produced by transesterification of any oils in the presence of alcohol using a catalyst. Most biodiesel production processes use vegetable oils as a feedstock, using a homogeneous catalyst. Using homogeneous catalyst has numerous limitations, including soap generation; inability to recover catalyst used, treatment of wastewater etc. and this elevates the overall production costs. Due to this limitations, heterogeneous catalysts are being used as a replacement. Heterogeneous catalysts are eco-friendly, and makes catalyst recovery easier hence reducing the total cost of production (Betiku et al., 2019; Obahiagbon & Ahonkhai, 2023). Also, a long term dependence on edible oil as feedstock, would lead to shortage of edible oil supply and hence, non-edible oil would be preferred for production (Balajii & Niju, 2020; Dharma et al., 2016).

Africa oil bean seed (*Pentaclethra macrophylla*) is a legume with no specific variety. Within Nigeria, it is found majorly in the southern part. It is well branched, forming crown-

like canopy. It flowers between the first quarter of the year, and after which the pods open by explosive mechanism, dispersing the seeds and the curls up. The pods are dark brown in colour and woody when matured and the seeds are dorsoventrally flattened, hard, and light brown in colour and about 3cm wide and 6cm long. The mesocarp of *P. macrophylla* seed serve as food, eaten as snack or dessert (Ndukwu & Onyeoziri, 2022). African oil bean seeds can be used to produce low cost and readily available oil for pharmaceutical and industrial applications by extracting oil from the seeds (Aremu & Ogunlade, 2016).

The catalyst used for biodiesel production in this study is created from antelope bone and the Africa oil bean seed pods. Antelope bones which contribute to large amount of bones pollution that occur within the world (Nasrollahzadeh et al., 2020) and Africa oil bean seed pods which is a waste material has been an environmental burden. Using both antelope bones and Africa oil bean seed pods as catalyst has various advantages including; minimization of waste produced by these materials, easiness to separate from the biodiesel produced and overall lower costs for the production process. Animal bones contain alkali metal oxides and have been widely used by previous researchers and have resulted in high yield of biodiesel (Adepoju et al., 2021; Mahmood et al., 2020; Obadiah et al., 2012).

Biodiesel production is a multi-parametric process dependent on multiple variables. The yield of biodiesel can be influenced by numerous process variables such as reaction time, temperature, type of catalyst, amount of catalyst, alcohol to oil ratio, agitation speed, moisture content etc. (Marinković et al., 2022). These variables affecting the production process could be optimized using tools like response surface methodology (RSM) and artificial neural network (ANN) to ensure an increase in the yield of biodiesel (Ayoola et al., 2019; Costarrosa et al., 2018). This provides for an opportunity to improve the economics of the process.

This study sought to produce biodiesel from Africa oil bean seed oil using a catalyst developed from antelope bones and Africa oil bean seed pod. RSM and ANN were used for modelling and optimization of the biodiesel production process.

Materials and Methods

Materials

Africa oil bean seed oil (AOBSO) and Africa oil bean seed pod (AOBSP) were gotten from Koko market, Warri-North local government, Delta state, Nigeria. The acid value, iodine value, saponification value, peroxide value, moisture content, density and pH of AOBSO is shown in Table 1. The antelope bones were gotten from Umoghun-Nokhua, a village in Orhionmwon local government of Edo state, Nigeria. The methanol and other reagents used for characterization of AOBSO and the biodiesel produced were of analytical grade and were obtained from a local vendor within Benin City, Edo state, Nigeria.

Table 1: Physiochemical properties of AOBSO

Properties (Unit)	Value
Acid value (mg KOH/g)	4.44
Iodine value (g I_2/100g)	81.6
Saponification value (mg KOH/g)	216
Peroxide value (meq/kg)	12
Density (g/cm^3)	0.875
pH	6.76

Catalyst Preparation

The antelope bones were washed thoroughly with water to remove any form of blood and dirt from it. Then, the washed antelope bones were sun dried for over a week and oven dried for 5 hours at 100^{o}C. After drying, the antelope bones were grinded using a grinding machine. The grinded antelope bone was then sieved using a mesh sieve to ensure particle uniformity. The powdered antelope bones were then calcined in a muffle furnace at 900^{o}C for 5 hours to give calcined antelope bone (CAB), and placed in a desiccator.

AOBSP was washed and then sun dried to remove any form of moisture within it. The sun dried AOBSP was oven dried at 100^{o}C for 4 hours. Then, AOBSP was grinded also using a grinding machine. After grinding, it was then sieved using a mesh sieve to ensure particle uniformity. The powdered AOBSP was then calcined in a muffle furnace at 700^{o}C for 5 hours to give calcined AOBSP (CAOBSP), and placed in a desiccator.

For the synthesis of the catalyst, wet impregnation method was used. Both CAB and CAOBSP were mixed in the same proportion together in distilled water to form a slurry solution. The resulting mixture was placed on a hot plate magnetic stirrer at 80^{o}C at a constant mixing rate till the water present was evaporated. The resultant particles were sun dried for several hours and oven dried at 120^{o}C. The solid dried powdered mixture was then subjected to further calcination at 900^{o}C for 4 hours to get a highly active heterogeneous base catalyst.

Catalyst Characterization

The synthesized catalyst and precursors made from antelope bone and AOBSP were characterized using Brunauer, Emmett and Teller (BET) analysis for surface area and pore properties determination. Fourier transform infrared (FTIR) spectroscopy analysis for bond structure and interaction, Scanning electron microscope (SEM) and energy dispersive X-ray (EDX) analysis showed the surface structure and elemental composition. Thermo-gravimetric (TGA)/differential thermal (DTA) analysis was used to show the thermal stability. X-ray fluorescence (XRF) analysis determined the composition of oxides. And X-ray diffraction (XRD) analysis indicated the crystalline phases.

Biodiesel Production

Based on the FFA (2.22%) of the AOBSO, a two-step transesterification process was used. Firstly, AOBSO went through an acid-catalyzed esterification process to get FFA content lower than 2%. The esterification pre-treatment step of the AOBSO was conducted using sulphuric acid and methanol. 2g of sulphuric acid was mixed with 150g of methanol. This mixture was added slowly to 500g of the AOBSO. The mixture was then agitated for 1 hour at 60^{o}C using a magnetic stirrer. After that, the mixture was separated into two layers in a separating funnel overnight. After which, the new FFA of the oil was determined.

Transesterification was carried out after following the procedure; A measured quantity of AOBSO was poured into a 250 ml conical flask and put on a hot plate magnetic stirrer, and heated to a set temperature. A particular quantity of catalyst was dissolved in a specific volume of methanol and then transferred into the AOBSO in the conical flask. The set values were according with the experimental data generated from the experimental design. At the end of the reaction, the mixture was poured into a separating funnel and left overnight to allow separation. The bottom layer contained glycerol, while the top layer contained biodiesel and unreacted methanol at separation. The resulting biodiesel was then washed thrice using hot distilled water to ensure removal of any impurities. The washed biodiesel was then dried in an oven and kept for further analysis. The yield of biodiesel produced was calculated using Equation (1) (Yusuff & Adesina, 2020).

$$\text{Biodiesel yield} = \frac{\text{mass of biodiesel produced}}{\text{mass of AOBSO used}} \times 100 \quad (1)$$

Experimental Design and Response Surface Methodology (RSM) Modeling

Box Behnken Design (BBD) was used to design the experiment using Design Expert 13. The effect of four independent variables (methanol/oil ratio, catalyst loading, reaction temperature and reaction time) on the biodiesel yield was investigated. The ranges of the process variables are shown in Table 2.

Table 2: Process variables and their lower, middle and upper limits

Factor	Process variable	Units	Lower	Middle	Upper
A	Methanol/oil ratio	mol/mol	6	12	18
B	Reaction time	min	50	85	120
C	Reaction temperature	^oC	50	60	70
D	Catalyst loading	(%wt)	1	2	3

The relationship of the process variables and the response is given by a second-order polynomial as shown in Equation (2). Equation (2) is a quadratic regression model fitted to the experimental data specifications generated from 29 runs created by BBD. The model terms were calculated using various regression analysis while analysis of variance (ANOVA) was used to assess the significance of the model terms.

$$Y_i = b_o + \sum b_i X_i + \sum b_{ij} X_i X_j + \sum b_{ii} X_i^2 + e_i \quad (2)$$

Where, Y_i denotes the predicted response, $b_o$is the value at intercept, $b_i$is the coefficient of first order, b_{ii} is the quadratic effect coefficient, $b_{ij}$is the interacting effect coefficient, X_i and X_j are the process variables that affect the response, and $e_i$is the experimental random error (Amenaghawon et al., 2022).

ANN Modeling

Data generated from BBD was used to train the ANN in order to make out a network that can be suitable and effective in modeling the biodiesel production process and plot the input variables onto the output variable. ANN modeling was done using Neural Power 2.5, a commercial ANN tool. Four nodes at the input layer, representing four process variables, two hidden layers, and one node at the output layer, representing the single response (biodiesel yield), made up the network architecture employed. The best transfer function was determined by testing various transfer functions, including Sigmoid, Gaussian, Hyperbolic tangent, Bipolar linear, Threshold liner, and linear functions, iteratively at 10000 epochs. The best network topology was determined on the basis of the coefficient of determination (R^2 value) and root mean square error (RMSE).

Results and Discussion

Catalyst Characterization

BET Analysis

The BET surface area is the main indicator for the surface properties of a catalyst. It shows the structure of the pores and the outer surface of a catalyst. Higher surface area and pore size gives active sites adequate room to attach to and for transesterification to take place (Madai et al., 2020). It can be seen that the surface area of the catalyst is larger than that of the precursor materials with CAOBSP having a surface area of 123.7 m^2/g, CAB having 188.8 m^2/g and the catalyst having 235.8 m^2/g. The catalyst was also characterized by a higher pore size and diameter of 0.1219 cc/g and 3.020nm respectively.

FTIR Analysis

The FTIR spectra of CAOBSP, CAB, and the catalyst are shown in Figure 1. AOBSP spectrum as seen in Figure 1a shows specific peaks at 3955.78cm^{-1}, 3666.02cm^{-1}, 2654.33cm^{-}

[1], 2100.04cm^{-1}, and 1804.32cm^{-1}. CAB as shown in Figure 1b, shows peaks at 3998.54cm^{-1}, 3698.64cm^{-1}, 2001.64cm^{-1}and 1500.88 cm^{-1}. And as seen in Figure 1c, the peaks for the catalyst occurred at 394.35cm^{-1}, 3655.78cm^{-1}, 2698.63cm[1], 1792.89cm^{-1} and 1492.88cm[1]. The peaks observed can be attributed to the O-H stretching vibration overlapped with fingerprint absorption of the molecule, presence of aromatic phosphate group arising from P=O stretch and also attributed to the presence of transitional metals carbonyl group.

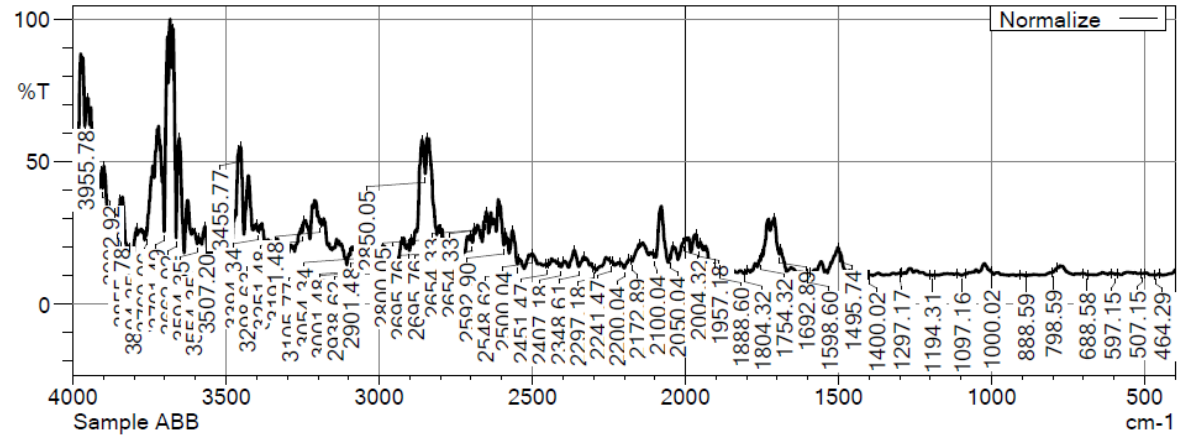

(a)

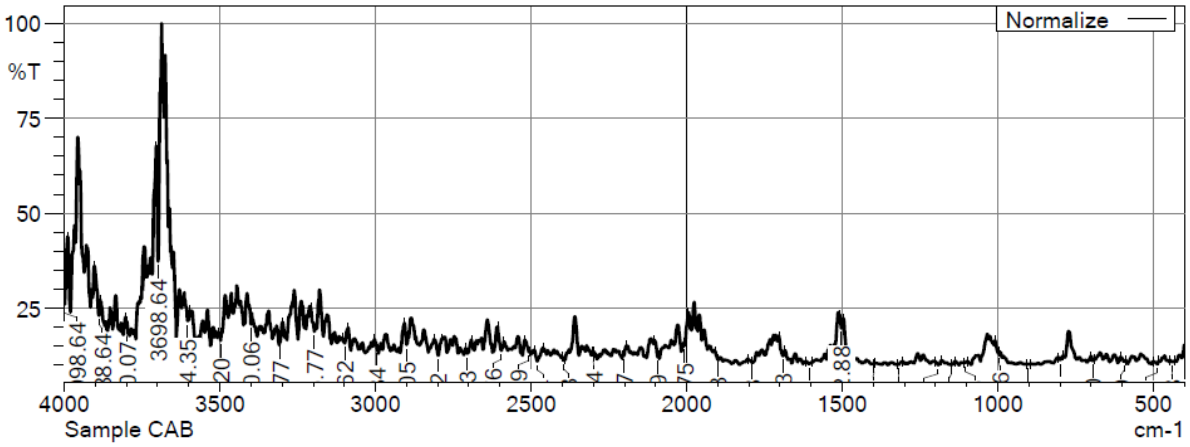

(b)

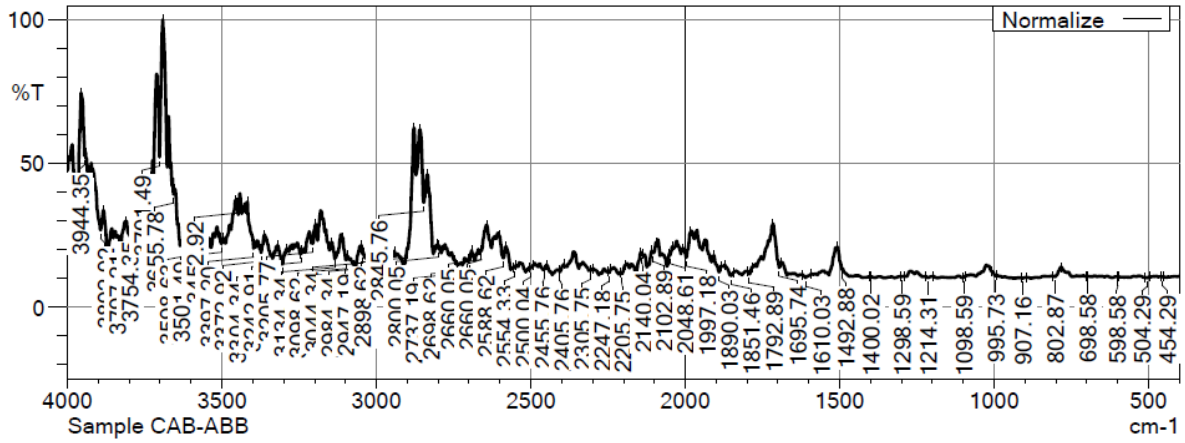

(c)

Figure 1: FTIR spectra of (a) CAOBSP (b) CAB (c) catalyst

SEM-EDX Analysis

The surface morphology of CAOBSP, CAB and the catalyst are shown in Figure 2. The pores of CAB as shown in Figure 2b are seen to be clumped together with no visible pores. CAOBSP image shown in Figure 2a, shows the pores are visible. For the catalyst shown in Figure 2c, good pores are seen which indicates available surface area making it good for its usage as a catalyst. Its larger surface area is favorable to the biodiesel production process as this gives more space for the reactants to attach.

The EDX results of both precursors and the catalyst can be seen in Figure 3. The composition of metals and other elements present in both precursors and the catalyst are shown in Table 3. The result shows that CAOBSP contains carbon and potassium while CAB contains calcium, phosphorus and carbon. Also, the catalyst contained calcium, phosphorus and carbon. The metals present in the catalysts are very active and this makes it an effective catalyst for biodiesel production.

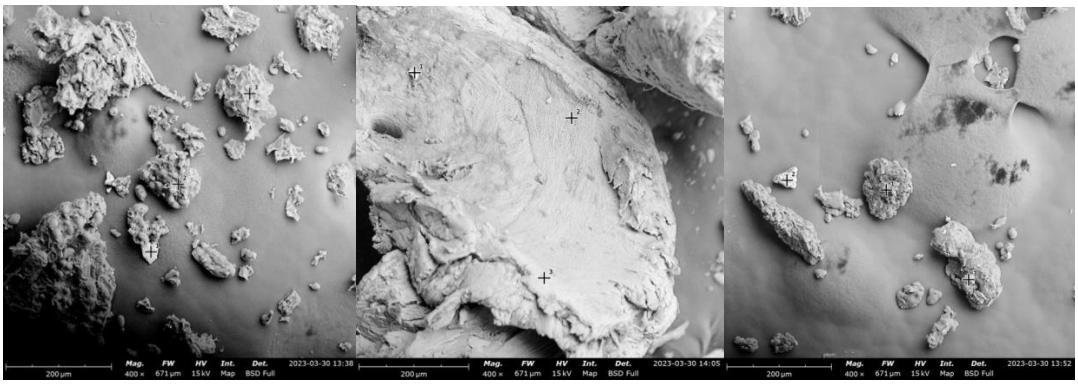

(a) (b) (c)

Figure 2: SEM image of (a) CAOBSP (b) CAB (c) catalyst

Table 3: Elemental composition of CAOBSP, CAB and the catalyst obtained from EDX

Element Number	Element Symbol	Element Name	Weight Concentration		
			CAOBSP	CAB	Catalyst
8	O	Oxygen	65.00	66.63	36.63
6	C	Carbon	13.07	2.45	5.29
19	K	Potassium	21.93	0.00	0.00
7	N	Nitrogen	0.00	10.84	0.00
20	Ca	Calcium	0.00	12.46	41.06
15	P	Phosphorus	0.00	7.63	17.02

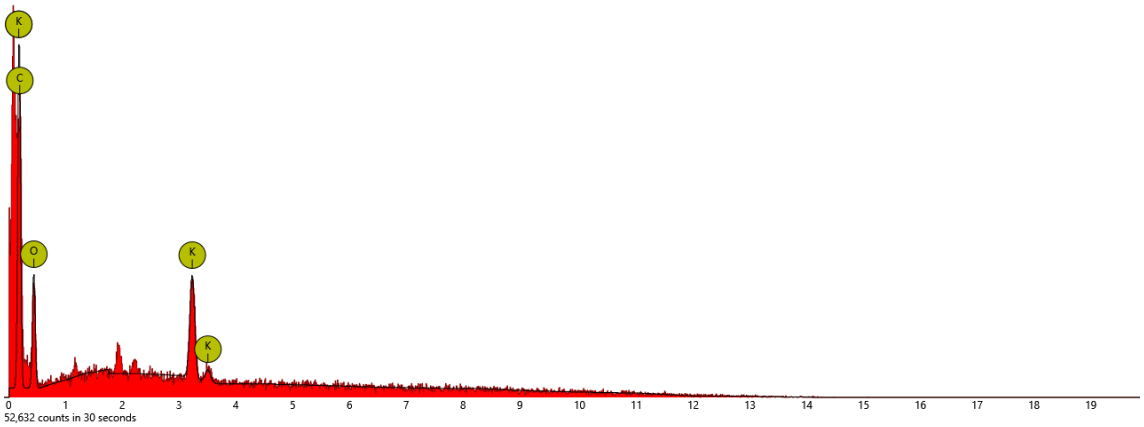

(a)

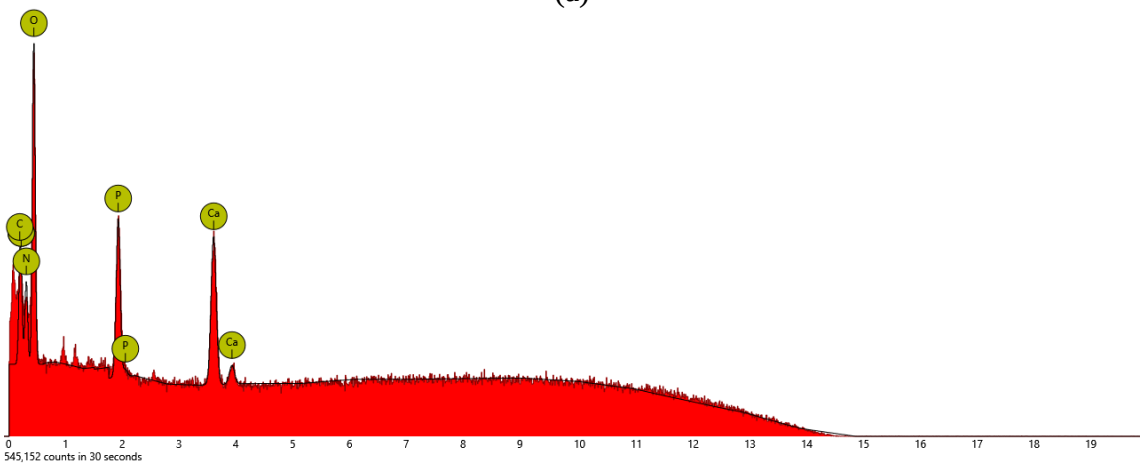

(b)

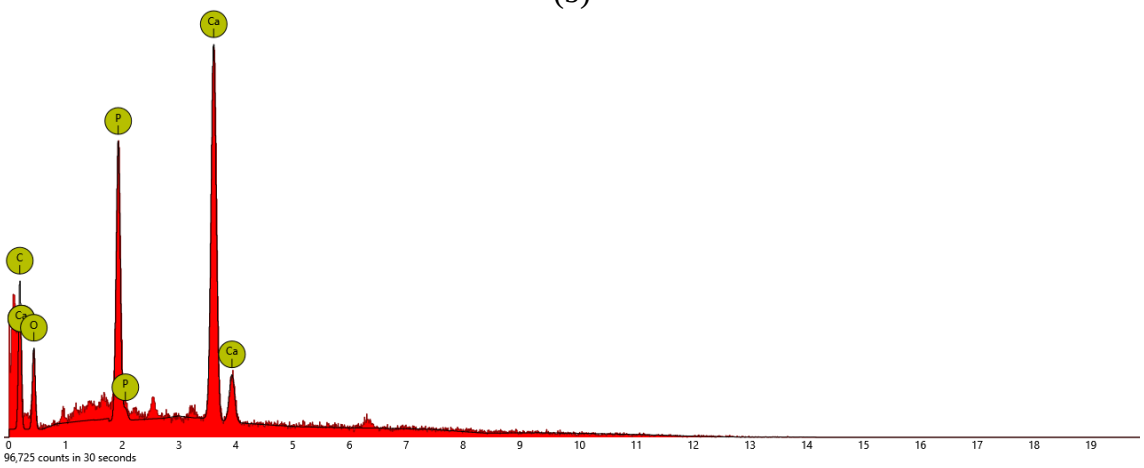

(c)

Figure 3: EDX patterns of (a) CAOBSP (b) CAB (c) catalyst

TGA/DTA Analysis

The TGA/DTA result for CAOBSP, CAB, and the catalyst can be seen in Figure 4. For CAOBSP, CAB and the catalyst, a significant decrease in weight can be noticed between 300^{o}C and 400^{o}C. This weight loss could be due to the removal of organic materials during the drying and calcination process. The maximum point of the DTA curve occurred around 600^{o}C for both precursors and catalyst.

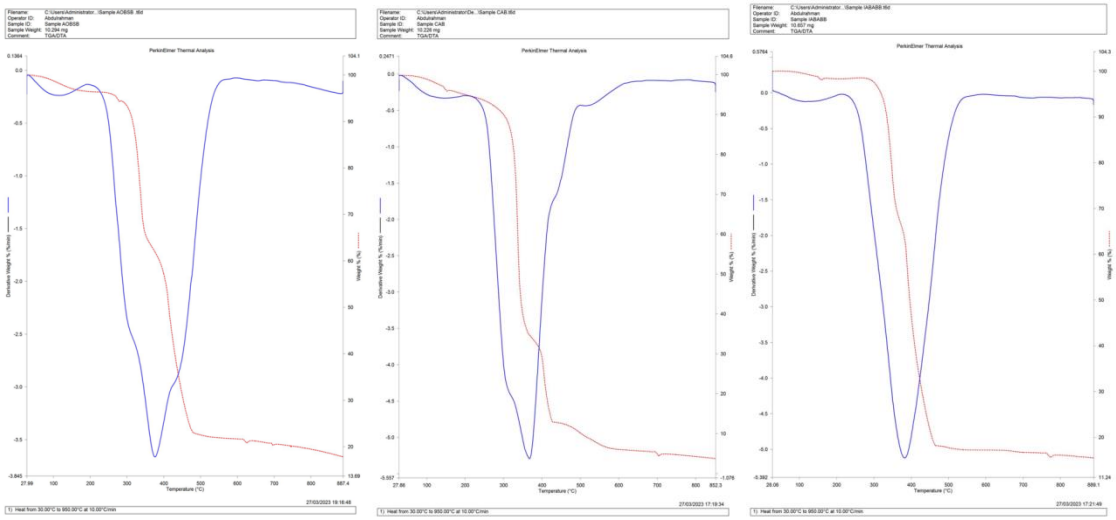

(a) (b) (c)

Figure 4: TGA/DTA results for (a) CAOBSP (b) CAB (c) catalyst

XRF Analysis

The oxides present in both precursors and catalyst are shown in Table 4. From the result, K_2O is the major constituent of CAOBSP while CAB and the catalyst had CaO as their major constituent. The catalyst had CaO has its major constituent concentration making it a good base catalyst for biodiesel production. The result also confirms the presence of both precursors in the catalyst.

Table 4: XRF analysis result for CAOBSP, CAB and the catalyst

Component	Element Concentration (%)		
	CAOBSP	CAB	Catalyst
SiO_2	3.206	0.365	3.700
V_2O_5	0.020	0.035	0.008
CR_2O_3	0.015	0.000	0.017
MnO	0.230	0.032	0.121
Fe_2O_3	1.318	0.181	0.453
Co_3O_4	0.018	0.003	0.000
NiO	0.131	0.000	0.011
CuO	0.108	0.031	0.044
Nb_2O_3	0.014	0.004	0.005
MoO_3	0.006	0.004	0.004
WO_3	0.000	0.008	0.004
P_2O_5	2.122	31.632	23.579
SO_3	8.583	0.120	0.858
CaO	12.306	60.467	50.879
MgO	7.770	2.886	5.072
K_2O	53.949	0.705	10.157
BaO	0.000	0.045	0.000
Al_2O_3	4.066	1.851	2.672
Ta_2O_5	0.008	0.014	0.012
TiO_2	0.281	0.000	0.076
ZnO	0.025	0.012	0.013
Ag_2O	0.017	0.027	0.019

Cl	2.046	1.208	0.823
ZrO_2	0.060	0.017	0.021
SnO_2	3.698	0.352	1.497

XRD Analysis

Figure 5 shows the XRD pattern for CAOBSP, CAB, and the catalyst. The high spectrum shows the crystallinity of both precursors and the catalyst. The 2θ value of the samples is seen to be in the range of 2–70º. The main characteristic peaks of CAOBSP are attributed to the presence of orthoclase, lime, vermiculite, anhydrite, sylvine, englishite and quartz. For CAB, the peaks are attributed to the presence of hydroxylapatite, lime, calcite, vermiculite, muscovite ad quartz. The peaks for the catalyst are attributed to the presence of hydroxylapatite, calcite, lime, quartz, vermiculite, and muscovite.

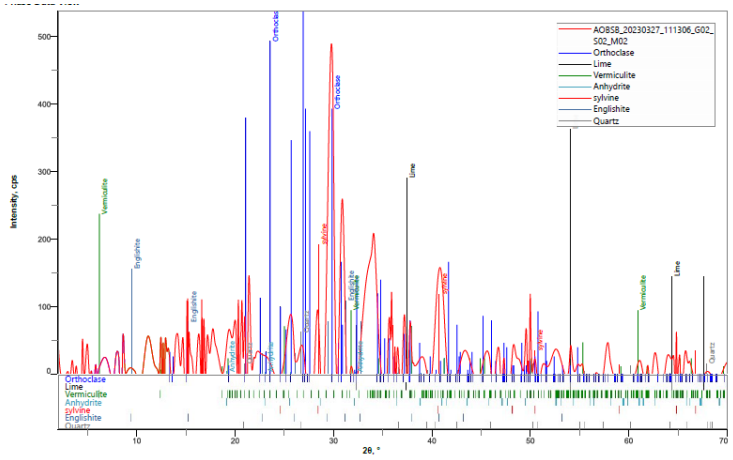

(a)

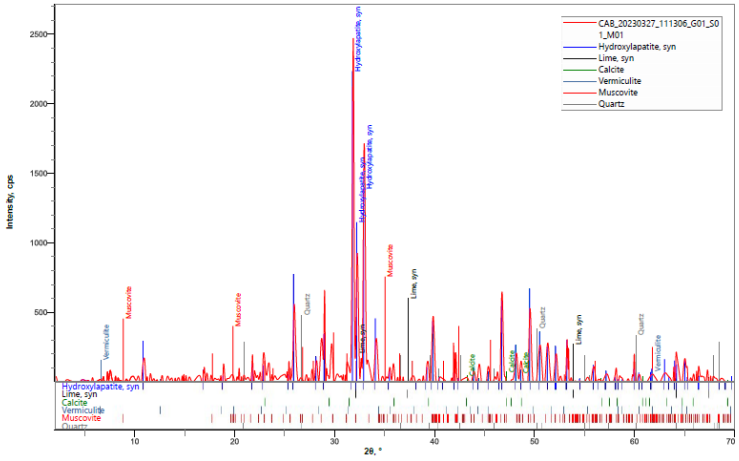

(b)

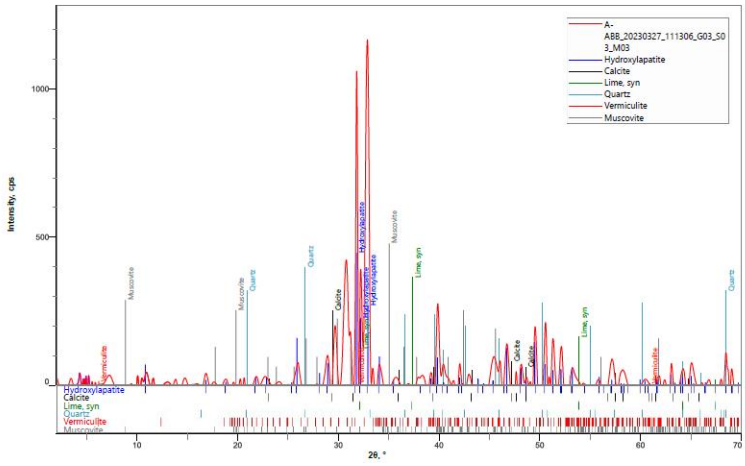

(c)

Figure 5: XRD pattern for (a) CAOBSP (b) CAB (c) catalyst

Optimization by RSM

The design of experiments involving reaction parameters where coded as A, B, C, and D. Table 5 shows transesterification reaction of AOBSO to produce biodiesel with the experimental and predicted responses.

Table 5: BBD experimental design with experimental yield, RSM and ANN predicted yield

Run	A:Methanol: Oil Ratio	B:Reaction Time	C:Reaction Temperature	D:Catalyst Loading	Experimental Yield	RSM Yield	ANN Yield
	mol/mol	min	^{o}C	(g)	%	%	%
1	12	120	70	2	81.85	80.89	81.85
2	12	85	60	2	91.64	92.98	92.98
3	12	50	60	3	78.98	77.96	78.976
4	12	85	70	3	78.01	78.31	78.021
5	6	50	60	2	82.00	82.48	82.00
6	12	85	50	1	81.78	82.82	81.78
7	6	85	50	2	83.26	84.09	83.259
8	12	85	50	3	81.68	81.54	81.683
9	12	85	60	2	92.84	92.98	92.98
10	12	50	50	2	80.33	86.36	80.33
11	12	85	60	2	92.54	82.51	92.98
12	12	85	70	1	84.88	83.27	84.88
13	6	85	60	3	82.00	82.51	82.00
14	18	120	60	2	82.41	83.27	82.41
15	12	85	60	2	93.24	92.98	92.98
16	12	120	60	1	82.40	83.27	82.399
17	18	85	60	1	89.01	92.98	89.011
18	18	85	60	3	81.54	83.70	81.54
19	12	85	60	2	94.64	92.98	92.98
20	6	85	60	1	89.31	87.09	89.31
21	12	50	60	1	85.00	85.54	85.00
22	12	120	50	2	84.85	84.24	84.85
23	18	85	70	2	84.51	83.96	84.51

24	18	85	50	2	85.01	84.56	85.01
25	6	120	60	2	87.00	86.67	87.002
26	12	50	70	2	84.33	83.32	84.33
27	18	50	60	2	83.64	85.31	83.639
28	12	120	60	3	82.20	81.95	82.196
29	6	85	70	2	84.26	85.00	84.26

From Table 5, the result obtained shows that the biodiesel yield for AOBSO ranged between 78.01% and 93.24%. Based on the data, the identified response surface model that relates the AOBSO biodiesel yield to the process variables in terms of coded factors and actual equation are given in Equation (3).

$$Y = +92.98 - 0.1425A + 0.5358B + 0.0775C - 2.33D - 1.56AB - 0.3750AC - 0.0400AD - 1.75BC + 1.45BD - 1.69\,CD - 3.09A^2 - 5.46B^2 - 5.49C^2 - 5.23D^2 \quad (3)$$

Where: Y = AOBSO biodiesel yield, A = methanol: oil ratio, B = reaction time, C = reaction temperature, D = catalyst loading.

Equation (3) given in terms of the coded factors A, B, C, and D can be used to make predictions about the response for given levels of each factor. By default, the high levels of the factors are coded as +1 while the low levels are coded as -1. The coded equation is useful for identifying the relative impact of the factors by comparing the factor coefficient. From equation (3); B, C, and BD are important in increasing the AOBSO biodiesel yield, whereas A, D, AB, AC, AD, BC, CD, A^2, B^2, C^2, and D^2 have a negative effect on the reaction, lowering the AOBSO biodiesel yield.

The AOBSO biodiesel yield to the process parameters (final equation) in terms of actual factors is shown in Table 6.

Table 6: Biodiesel yield equation in terms of actual factors

Yield	=
-217.92957	
+3.05472	METHANOL:OIL RATIO
+1.07882	REACTION TIME
+7.43375	REACTION TEMPERATURE
+25.30893	CATALYST LOADING
-0.007417	METHANOL:OIL RATIO * REACTION TIME
-0.006250	METHANOL:OIL RATIO * REACTION TEMPERATURE
-0.006667	METHANOL:OIL RATIO * CATALYST LOADING
-0.005000	REACTION TIME * REACTION TEMPERATURE
+0.041571	REACTION TIME * CATALYST LOADING
-0.169250	REACTION TEMPERATURE * CATALYST LOADING
-0.085822	METHANOL:OIL RATIO²
-0.004457	REACTION TIME²
-0.054896	REACTION TEMPERATURE²
-5.23458	CATALYST LOADING²

The equation in terms of actual factors can be used to make predictions about the response for given levels of each factor. Here, the levels should be specified in the original units for each factor. This equation should not be used to determine the relative impact of each factor because the coefficients are scaled to accommodate the units of each factor and the intercept is not at the center of the design space. Table 7 shows the summary of the model for AOBSO Biodiesel yield.

Table 7: Model Summary for Palm-kernel oil Biodiesel Yield

Source	Std. Dev.	R^2	Adjusted R^2	Predicted R^2	PRESS	
Linear	4.51	0.1237	-0.0224	-0.0870	606.03	
2FI	4.98	0.1998	-0.2447	-0.3552	755.60	
Quadratic	1.46	0.9468	0.8935	0.7297	150.68	Suggested
Cubic	1.52	0.9752	0.8845	-1.3303	1299.23	Aliased

Table 7 shows that the suggested quadratic model has the highest R^2 value of 0.9468 when compared to the other models with the exception of the aliased cubic model. The focus of model summary statistics is on the model maximizing the R-squared and predicted R-squared values. A higher R-squared value indicates a stronger model and good prediction of the responses. In this case, the value of R^2 was found to be 0.9468, which account for up to 94.68% of the response variability. Hence, the results of the analysis of variance (ANOVA) for the identified model are shown in Table 8 and Table 9.

Table 8: ANOVA for the Response Surface Quadratic Model

Source	Sum of Squares	df	Mean Square	F-value	p-value	
Model	527.86	14	37.70	17.78	< 0.0001	significant
A-METHANOL:OIL RATIO	0.2437	1	0.2437	0.1149	0.7396	
B-REACTION TIME	3.45	1	3.45	1.63	0.2231	
C-REACTION TEMPERATURE	0.0721	1	0.0721	0.0340	0.8564	
D-CATALYST LOADING	65.19	1	65.19	30.75	< 0.0001	
AB	9.70	1	9.70	4.58	0.0505	
AC	0.5625	1	0.5625	0.2653	0.6145	
AD	0.0064	1	0.0064	0.0030	0.9570	
BC	12.25	1	12.25	5.78	0.0306	
BD	8.47	1	8.47	3.99	0.0655	
CD	11.46	1	11.46	5.40	0.0356	
A^2	61.92	1	61.92	29.21	< 0.0001	
B^2	193.34	1	193.34	91.20	< 0.0001	
C^2	195.47	1	195.47	92.20	< 0.0001	
D^2	177.74	1	177.74	83.84	< 0.0001	
Residual	29.68	14	2.12			
Lack of Fit	24.85	10	2.48	2.06	0.2539	not significant
Pure Error	4.83	4	1.21			
Cor Total	557.54	28				

The Model F-value of 17.78 implies the model is significant. There is only a 0.01% chance that an F-value this large could occur due to noise. The P-values less than 0.0500 indicate model terms are significant. In this case D, BC, CD, A^2, B^2, C^2, D^2 are significant model terms. Values greater than 0.1000 indicate the model terms are not significant. If there are many insignificant model terms (not counting those required to support hierarchy), model reduction may improve your model. Also, the Lack of Fit F-value of 2.06 implies the Lack of Fit is not significant relative to the pure error. There is a 25.39% chance that a Lack of Fit F-value this large could occur due to noise. Non-significant lack of fit is good.

Table 9: ANOVA statistical parameter for Response Surface Quadratic Model

Std. Dev.	**1.46**
Mean	85.00
C.V. %	1.71
PRESS	150.68
R^2	0.9468
Adjusted R^2	0.8935
Predicted R^2	0.7297
Adeq Precision	14.3394

High R^2 value (0.9468) indicates that the fitted model predicts the AOBSO biodiesel yield with reasonable precision. The adjusted R^2 which also indicates the model's high significance is 0.8935. The Predicted R^2 of 0.7297 is in reasonable agreement with the Adjusted R^2 of 0.8935; i.e. the difference is less than 0.2. The coefficient of variation (1.71%) is relatively low, indicating that the model is reproducible.

The Adequate Precision measures the signal to noise ratio. A ratio greater than 4 is desirable. The ratio of 14.3394 indicates an adequate signal. This model can be used to navigate the design space. Within a given set of parameters, the model can be used to predict the responses. The predicted biodiesel yield and oil conversion values for biodiesel production from AOBSO are plotted with the actual values and the results of the plot are shown in Figure 6. It can be seen from both plots that the data points are close to the diagonal line which indicates that the predicted and actual responses were very close and justifies the fitness of the model to accurately predict biodiesel yield and oil conversion.

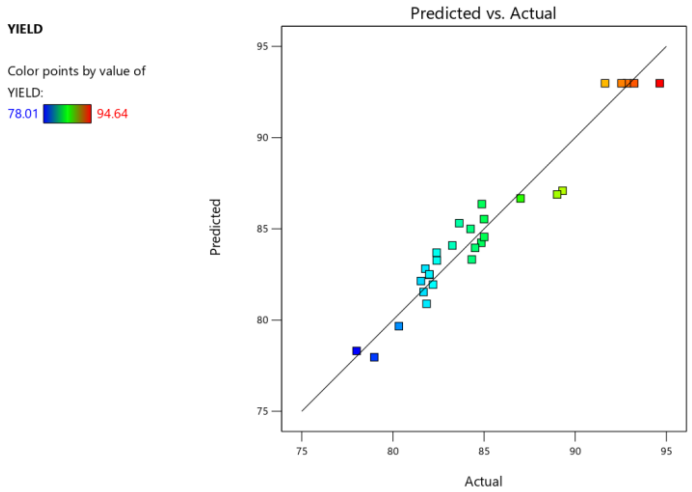

Figure 6: Predicted and experimental biodiesel yield

Effect of process variables on AOBSO biodiesel yield

Figure 7 shows the interaction between biodiesel yield, and other process variables on a 3D surface model plot. For reaction time, a gradual increase at the early stage of the transesterification resulted in an increased overall yield of biodiesel until it gets to 85 minutes after which further increase in the reaction timing reduced the yield. An increasing methanol: oil ratio at the beginning of the reaction resulted in an increased overall yield of biodiesel until it gets to 11.8 mol/mol after which an increase in this ratio resulted in a reduction in biodiesel yield. A gradual increase in the temperature at the early stage of the reaction resulted in an initial increase in the overall yield. This interaction was sustained till the temperature reached 60^{o}C, after which further increase in temperature slightly reduced biodiesel yield. Also, as seen

in the 3D plots, a gradual increase in the catalyst loading at the early stage of the reaction resulted in an initial increase in the yield. And this increase continued till the catalyst loading reached 1.773 wt%, after which further increment in catalyst loading reduced the yield. At 85.5 minutes, 11.8 mol/mol methanol: oil ratio, 60^{o}C and catalyst loading of 1.773 wt%, an optimum yield of 93.2523% was obtained.

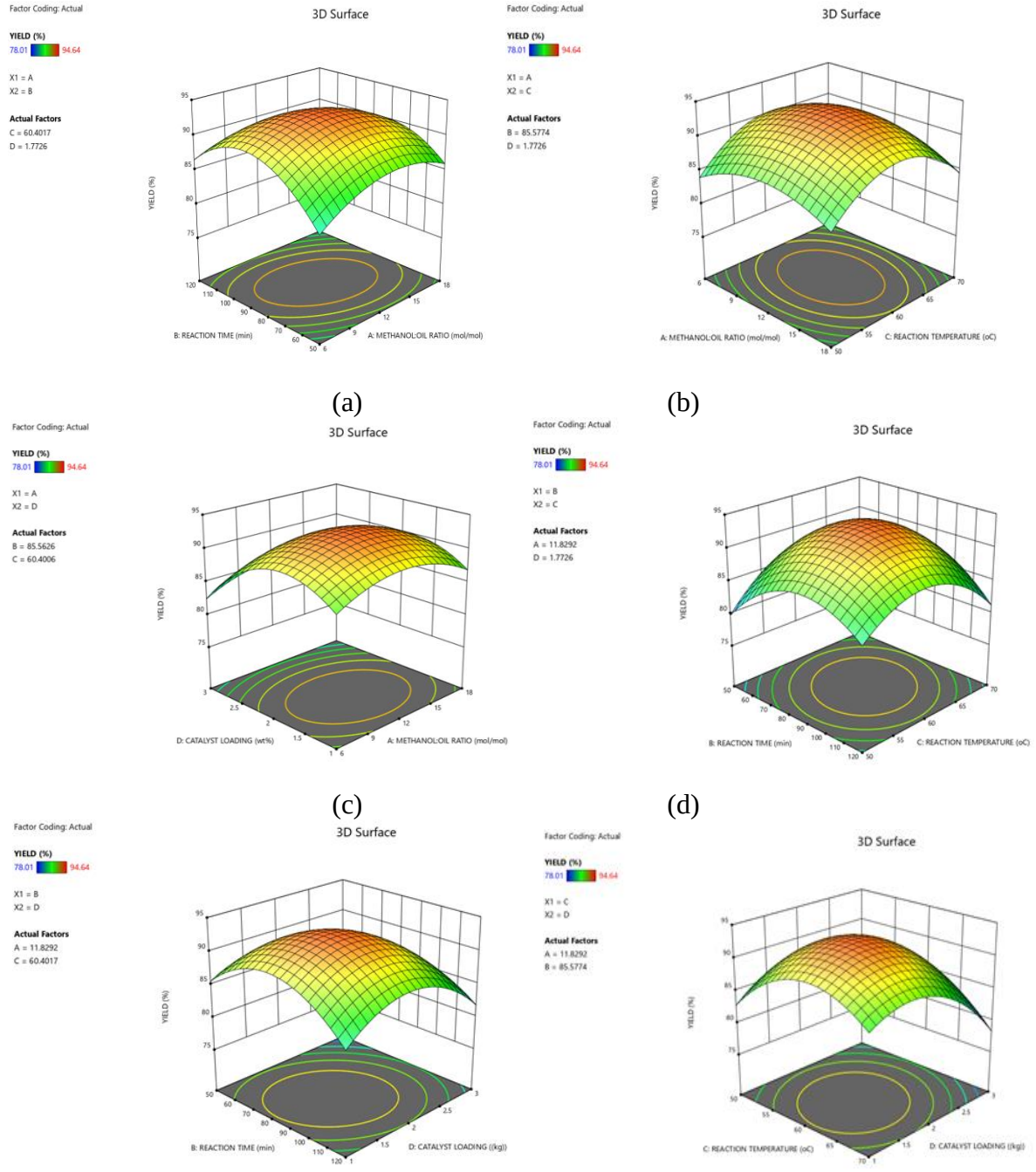

Figure 7: 3D surface plots showing interaction between (a) methanol: oil and reaction time (b) methanol: Oil and reaction temperature (c) methanol: oil and catalyst loading (d) reaction time and reaction temperature (e) reaction time and catalyst loading (f) reaction temperature and catalyst loading

Optimization Using ANN

Optimum Training Algorithm

Selection and testing of neural network includes selecting the best architectures (Multilayer Normal Feed Forward MNFF and Multilayer Full Feed Forward MFFF) and topology of the ANN (number of neurons in the hidden layer, transfer functions for both the hidden and output layers) produced estimation and prediction of oxalic acid concentration. Table 10 shows the various R^2 and RMSE values for different transfer functions, acquired from various trainings and the Tanh gave the highest R^2 and corresponding lowest RMSE values.

Table 10: R^2 and RMSE for Various Transfer Functions

Transfer Function	RMSE	R^2
Sigmoid	1.5283	0.8827
Tanh	0.41542	0.99133
Gaussian	0.87373	0.96166
Linear	4.1773	0.12368
Threshold Linear	3.154	0.50043
Bi polar Linear	4.1689	0.12718

From the training process shown in Table 11, the Quick Prop (QP) with (R^2 value of 0.99131 and RMSE, 0.41586) was the best training method for predicting the optimal biodiesel yield. Iterations on the various transfer functions were also performed to establish the best network topology. The optimal number of neurons for the network was also determined using the best transfer function. When compared to all other transfer functions, the QP model produced superior R^2 values.

Table 11: R^2 and RMSE values of MNFF and MFFF using different training algorithms

Connection type	Learning algorithm	RMSE	R^2
MNFF	IBP	0.41963	0.99116
	BBP	0.4648	0.98915
	QP	0.41671	0.99128
	GA	0.91046	0.95837
	LM	2.887	0.58143
MFFF	IBP	0.41677	0.99128
	BBP	0.46337	0.98922
	QP	0.41586	0.99131
	GA	0.74473	0.97215
	LM	--	--

Figure 8 shows the network topology of the neural network used for this study. Two hidden layers with four (4) nodes were adequate and subsequently adopted for the best training process. Figure 9 denotes the plots of the number of neurons and the R^2 values. For MFFF, 4 nodes were the minimum number of nodes required for a best fitted model.

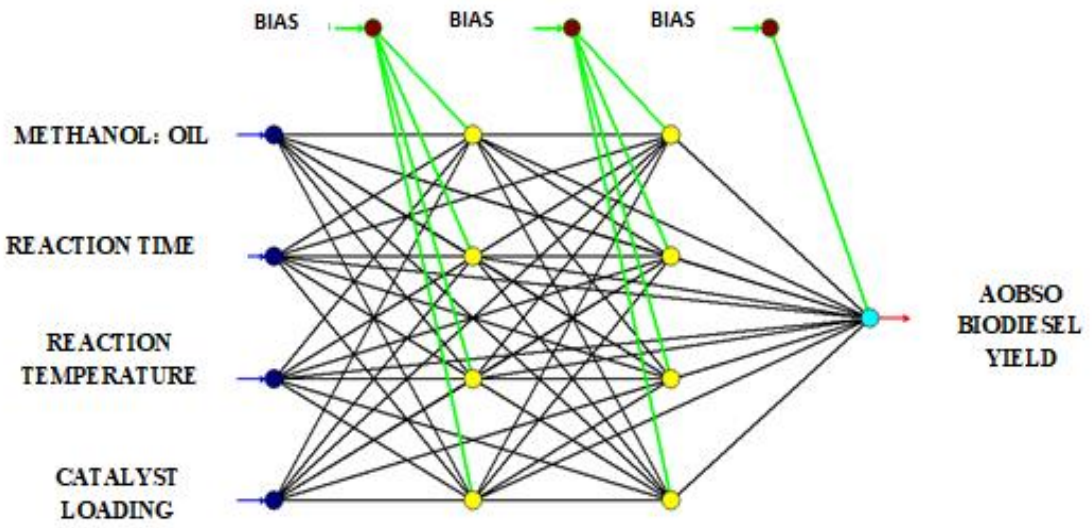

Figure 8: Architecture of the Neural Network

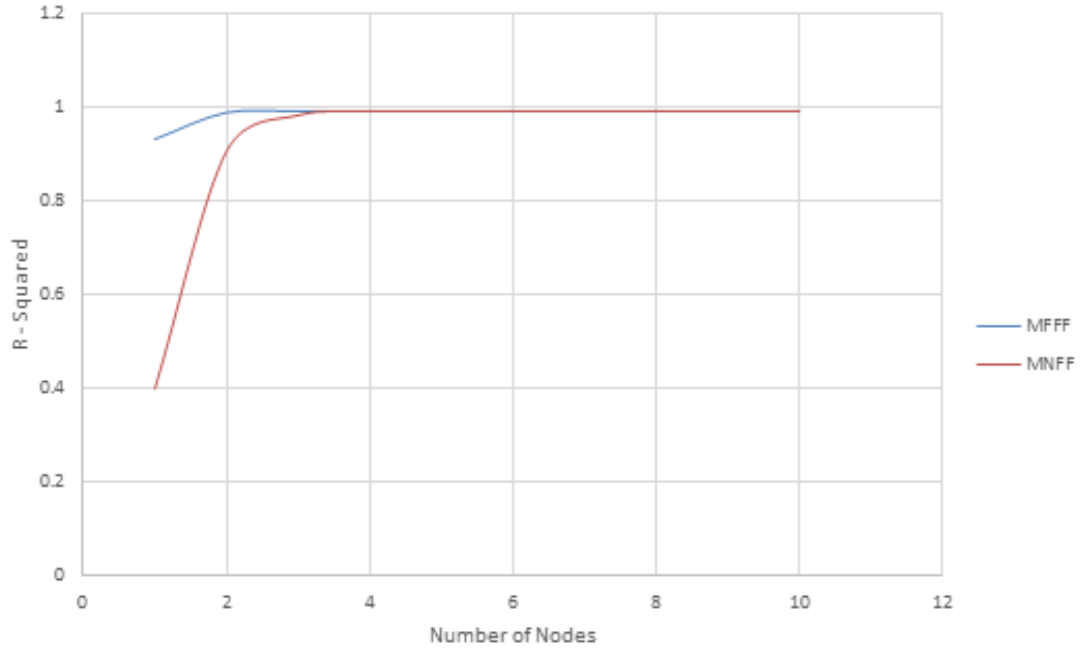

Figure 9: R^2 values and corresponding number of neurons for MNFF and MFFF using Hyperbolic-Tangent function

Verification OF ANN Model Result

Table 5 shows how closely the predicted values from ANN fit the experimented data. This means that the empirical model derived using ANN was able to accurately describe the relationship between the input variables and AOBSO biodiesel yield obtained

Optimization Results from the ANN Model

The optimum values shown in Table 12 were determined using the following conditions; QP, and Tanh, connection type of MFFF with four nodes and two hidden layers. After proper estimation, the maximum AOBSO biodiesel yield of 95.00862% was obtained at methanol: oil

ratio of 7.5229 mol/mol, reaction time of 57.0027 minutes, a reaction temperature of 56.2678 ^{o}C, and catalyst loading of 1.0474wt%.

Table 12: Optimum range of independent variables using ANN

	Max. 1	Max. 2	Max. 3	Max. 4	Max. 5
A	95.00116	94.96879	94.93709	94.92789	94.92617
A	7.20000	6.00000	8.40000	7.20000	9.60000
B	57.00000	57.00000	64.00000	64.00000	57.00000
C	56.00000	56.00000	58.00000	58.00000	56.00000
D	1.00000	1.00000	1.20000	1.20000	1.20000

Characterization of Biodiesel

Table 13 summarizes the various properties of AOSBO biodiesel produced. The values obtained were compared to ASTM D6751and EN14214 standards and were within specifications indicating that the biodiesel produced can be used. The acid value being low indicates low corrosiveness. The calorific value obtained indicates that it contains a lot of energy within. The flash point which is within specifications shows thermal stability making it safe for storage and transportation. The Low viscosity shows there would be good fuel flow, which makes fuel atomization during spraying easy.

Table 13: Summary of AOSBO biodiesel

Property	Value	ASTM D6751	EN 14214
Iodine value (g I_2/100g)	72.3	-	<120
Acid value (mg KOH/g)	0.41	0.5	0.5
Calorific value (MJ/kg)	35.35	-	>35
Flash point (^{o}C)	124	100-170	>120
Density (kg/m^3)	892	849	860-900
Viscosity (mm^2/s) at 40^{o}C	5.71	1.9-6	3.5-5

Conclusions

In this study, biodiesel from African oil bean seed oil in the presence of a heterogeneous base catalyst made from African bean seed pod and antelope bone. The results from characterization of the catalyst showed the presence of necessary metal oxides, high surface area and large pore diameter indicating suitability for it to be used as a catalyst. Also, the study evaluated two optimization tools (RSM and ANN) which revealed that a maximum yield of 93.2523% using RSM and a maximum yield of 95% using ANN. With higher R^2 value and lower RMSE value, ANN was chosen as a better optimization tool. Biodiesel produced at optimum conditions was within the specifications when compared with ASTM D6751 and EN 14214 standards.

References

Adekunle, A. S., Oyekunle, J. A. O., Oduwale, A. I., Owootomo, Y., Obisesan, O. R., Elugoke, S. E., Durodola, S. S., Akintunde, S. B., & Oluwafemi, O. S. (2020). Biodiesel potential of used vegetable oils transesterified with biological catalysts. *Energy Reports*, *6*, 2861–2871. https://doi.org/10.1016/j.egyr.2020.10.019

Adepoju, T. F., Ibeh, M. A., & Asuquo, A. J. (2021). Elucidate three novel catalysts synthesized from animal bones for the production of biodiesel from ternary non-edible and edible oil blend: A case of Jatropha curcus, Hevea brasiliensis, and Elaeis guineensis oil. *South African Journal of Chemical Engineering*, *36*(January), 58–73.

https://doi.org/10.1016/j.sajce.2021.01.002

Amenaghawon, A. N., Evbarunegbe, N. I., & Obahiagbon, K. (2021). Optimum biodiesel production from waste vegetable oil using functionalized cow horn catalyst: A comparative evaluation of some expert systems. *Cleaner Engineering and Technology*, *4*, 100184. https://doi.org/10.1016/j.clet.2021.100184

Amenaghawon, A. N., Obahiagbon, K., Isesele, V., & Usman, F. (2022). Optimized biodiesel production from waste cooking oil using a functionalized bio-based heterogeneous catalyst. *Cleaner Engineering and Technology*, *8*(April), 100501. https://doi.org/10.1016/j.clet.2022.100501

Aremu, A. K., & Ogunlade, C. A. (2016). Effect of operating parameters on mechanical oil expression from African oil bean seeds. *Global Journal of Science Frontier Research: D, Agriculture and Veterinary*, *16*(1), 19-26.

Ayoola, A. A., Hymore, F. K., Omonhinmin, C. A., Olawole, O. C., Fayomi, O. S. I., Babatunde, D., & Fagbiele, O. (2019). Analysis of waste groundnut oil biodiesel production using response surface methodology and artificial neural network. *Chemical Data Collections*, *22*, 100238. https://doi.org/10.1016/j.cdc.2019.100238

Balajii, M., & Niju, S. (2020). Banana peduncle – A green and renewable heterogeneous base catalyst for biodiesel production from Ceiba pentandra oil. *Renewable Energy*, *146*, 2255–2269. https://doi.org/10.1016/j.renene.2019.08.062

Betiku, E., Okeleye, A. A., Ishola, N. B., Osunleke, A. S., & Ojumu, T. V. (2019). Development of a Novel Mesoporous Biocatalyst Derived from Kola Nut Pod Husk for Conversion of Kariya Seed Oil to Methyl Esters: A Case of Synthesis, Modeling and Optimization Studies. *Catalysis Letters*, *149*(7), 1772–1787. https://doi.org/10.1007/s10562-019-02788-6

Costarrosa, L., Leiva-Candia, D. E., Cubero-Atienza, A. J., Ruiz, J. J., & Dorado, M. P. (2018). Optimization of the transesterification of waste cooking oil with mg-al hydrotalcite using response surface methodology. *Energies*, *11*(2), 302. https://doi.org/10.3390/en11020302

Dharma, S., Masjuki, H. H., Ong, H. C., Sebayang, A. H., Silitonga, A. S., Kusumo, F., & Mahlia, T. M. I. (2016). Optimization of biodiesel production process for mixed Jatropha curcas-Ceiba pentandra biodiesel using response surface methodology. *Energy Conversion and Management*, *115*, 178–190. https://doi.org/10.1016/j.enconman.2016.02.034

Madai, I. J., Chande Jande, Y. A., & Kivevele, T. (2020). Fast rate production of biodiesel from neem seed oil using a catalyst made from banana peel ash loaded with metal oxide (Li-CaO/Fe2(SO4)3). *Advances in Materials Science and Engineering*, *2020*. https://doi.org/10.1155/2020/7825024

Mahmood, H., Iqbal, T., Haider, C., & Javaid, A. (2020). Sustainable biodiesel production from waste cooking oil utilizing waste ostrich (Struthio camelus) bones derived heterogeneous catalyst. *Fuel*, *277*(April), 118091. https://doi.org/10.1016/j.fuel.2020.118091

Marinković, M., Waisi, H., Blagojević, S., Zarubica, A., Ljupković, R., Krstić, A., & Janković, B. (2022). The effect of process parameters and catalyst support preparation methods on the catalytic efficiency in transesterification of sunflower oil over heterogeneous KI/Al2O3-based catalysts for biodiesel production. *Fuel*, *315*(November 2021). https://doi.org/10.1016/j.fuel.2022.123246

Nasrollahzadeh, M., Soheili Bidgoli, N. S., Shafiei, N., Soleimani, F., Nezafat, Z., & Luque, R. (2020). Low-cost and sustainable (nano)catalysts derived from bone waste: catalytic applications and biofuels production. *Biofuels, Bioproducts and Biorefining*, *14*(6), 1197–1227. https://doi.org/10.1002/bbb.2138

Ndukwu, M. C., & Onyeoziri, C. I. (2022). African oil bean seed as feedstock for bio-oil and

biodiesel production and on the effects of thermal pre-treatments on the quality of the bio-oil. *Biomass Conversion and Biorefinery*, *12*(7), 2799–2810. https://doi.org/10.1007/s13399-020-00754-6

Obadiah, A., Ajji, G., Vasanth, S., & Raman, K. (2012). Bioresource Technology Biodiesel production from Palm oil using calcined waste animal bone as catalyst. *Bioresource Technology*, *116*, 512–516. https://doi.org/10.1016/j.biortech.2012.03.112

Obahiagbon, K., & Ahonkhai, D. O. (2023). Optimized Biodiesel Production from Waste Cooking Oil Using Nickel (II) Nitrate Doped Chicken Manure as Catalyst. *European Journal of Applied Sciences*, *11*(3), 812–824. https://doi.org/10.14738/aivp.113.14891

Odetoye, T. & Amusan, G. (2019). Cocoa pod ash as biodiesel catalyst for biodiesel production from waste chicken fat. *CIGR Journal*, *21*(4), 141–151.

Ogunsola, A. D., Durowoju, M. O., Alade, A. O., Jekayinfa, S. O., & Ogunkunle, O. (2022). Modeling and optimization of two-step shea butter oil biodiesel synthesis using snail shells as heterogeneous base catalysts. *Energy Advances*, *2*, 113–128. https://doi.org/10.1039/d1ya00042j

Okonkwo, C. P., Ajiwe, V. I. E., Ikeuba, A. I., Emori, W., Okwu, M. O., & Ayogu, J. I. (2023).Production and performance evaluation of biodiesel from Elaeis guineensis using natural snail shell-based heterogeneous catalyst: kinetics, modeling and optimisation by artificial neural network . *RSC Advances*, *13*(28), 19495–19507. https://doi.org/10.1039/d3ra02456c

Yusuff, A. S., & Adesina, O. A. (2020). Biodiesel synthesis from palm olein oil using anthill as catalyst. *Journal of Chemical Technology and Metallurgy*, *55*(2), 300–306.